

Appendix B

Spectrometer Design

B.1 Spectrometer

A great deal of work has been devoted to the design of the spectrometer since the proposal. The spectrometer consists of two toroidal magnets, each with 7 coils equally spaced around the azimuth, which focus the Møller electrons radially and azimuthally at the detector plane. As described in the original proposal, the spectrometer makes use of the fact that we are considering identical-particle scattering. Thus we obtain 100% azimuthal acceptance by accepting backward scattered Møllers, which have lab scattering angles of 5.5-9.5 mrad, and forward-scattered Møllers from 9.5-17 mrad in a particular phi bite (open sector), leaving the diametrically opposed phi bite available for placement of the coils (closed sector). The upstream magnet, despite the small radial size compared to its length along the beamline, is a conventional toroidal magnet. The downstream magnet is a novel design, the geometry of which helps to focus Møller electrons with a large range of scattered angles and energies (5.5-17 mrad and 2.5-9.5 GeV).

Most of the work that has been done was for the hybrid magnet, although the upstream torus has also been updated with a realistic conductor layout. The hybrid magnet has undergone several iterations using a commercially available software package available from Vector Fields, called TOSCA, to design the coils and produce fields maps, which are then imported into a GEANT4 simulation which includes radiative losses. The first step was verification of the field used in the proposal, both through direct comparison of the fields and in the result of GEANT simulations. The design of both magnets now includes suggestions made by engineers during the first engineering review, held on August 31, 2010, which will be discussed in Section B.4. The current design is shown in Figure B.1. There is now a design which includes an actual conductor layout with reasonable electromagnetic and water-cooling properties, which is being optimized for desirable optics properties while staying within the engineering constraints.

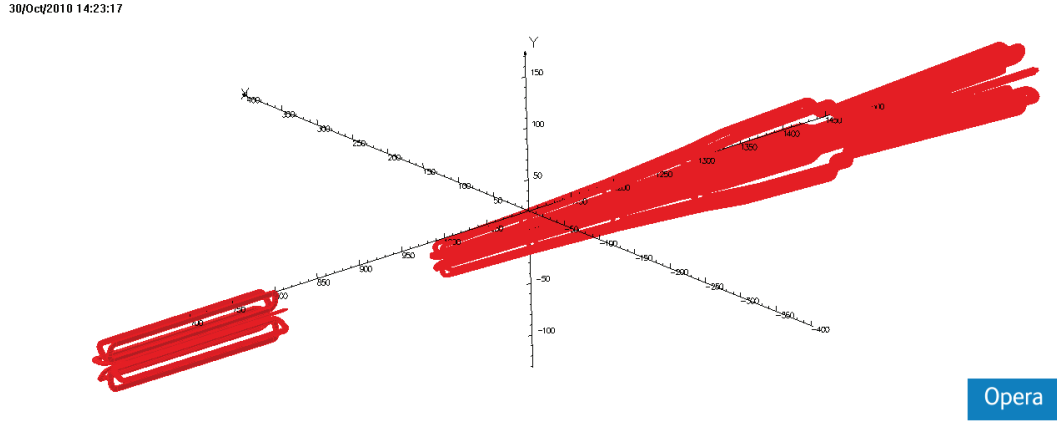


Figure B.1: Current design of the spectrometer which was developed using TOSCA.

B.2 Verifying the Proposal Field

The field map that was used in the proposal was generated with a “home-built” code, written expressly for the optimization of the hybrid spectrometer. It is a great success that the map was reproduced independently using TOSCA, and the values of the fields in the two maps can be directly compared. There are 3 components to the field (B_x , B_y and B_z) at each individual point in space, so it is difficult to show the agreement here with limited space. The individual cartesian components of the field, in bins of radius vs. azimuthal angle, ϕ , for a z location 12 m downstream of the target is shown in Figure B.2. The field gets large near the physical locations of the coils, and in the original proposal map there are some discontinuities which occur for the calculation of the field within the location of the coils. The TOSCA calculation appears more smooth.

In this sector B_x is primarily the azimuthally focusing component, and B_y the radially focusing component. The component in the z direction is very small. It should be noted that, because this is not a perfect toroid, the field components vary as a function of ϕ for a given radius. This affects our ability to radially focus Møllers that are scattered at large azimuthal angles. In addition, near the outer radius the field is azimuthally de-focusing. Because most of the tracks pass through the upstream torus between the low radius parts of the coils, the upstream torus focuses them azimuthally, and this effect is exploited in the design of the spectrometer.

Figure B.3 shows the excellent agreement between even the relatively small azimuthally (de-)focusing component of the field (left) between the two maps at a radial location of 15 cm, in 5° bites in ϕ vs. z . The right shows the agreement for the radially focusing component. The red points are from the original proposal map, and the black points are from the TOSCA map. There is a bit more spread in the field values from the proposal map at ϕ values close to the coils (which are centered

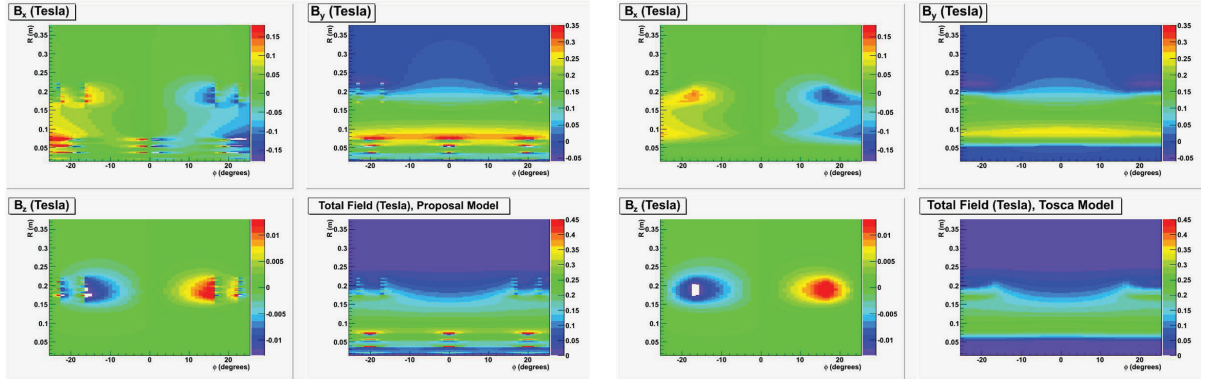


Figure B.2: Plots of the cartesian field components (B_x , B_y and B_z as well as the total field) in one sector for the original proposal magnetic field map (left) and TOSCA version of the proposal map (right). The field values are plotted in bins of R vs. ϕ for a z location of 12 m from the center of the target.

at $\pm 25^\circ$), consistent with what is shown in Figure B.2.

Reproducing the proposal field in TOSCA had a dual purpose. One was to check that the assumptions made with the field map produced for the proposal were valid. The other was to gain experience with using TOSCA. There were slight differences in the fields due to actual differences in the coil geometry as defined in the code used to calculate the proposal model compared to TOSCA (see Figure B.4). The proposal model used line currents, and the coils in TOSCA are defined as trapezoidal blocks. The overall agreement was quite good, with the largest differences less than 10% where the geometry differed significantly. Further effort to make the models agree more closely would likely be wasted, mostly due to the difficulty of defining the coils in TOSCA compared to the way they were done in the proposal model.

In addition to direct comparison of the fields, maps were produced in TOSCA which could then be read into the GEANT4 simulation. While tracking of scattered particles with an energy dependence on scattering angle is relatively easy in TOSCA, the GEANT4 simulations are necessary to incorporate energy loss in the target and other radiative effects. Some results of the simulation are shown in Figure B.5 for tracks at the focal plane, which is located 28.5 m downstream of the center of the target. Again, the agreement between the simulations using the two fields was quite good, and further work to reproduce the proposal field was abandoned in order to move forward with the design of more realistic coils.

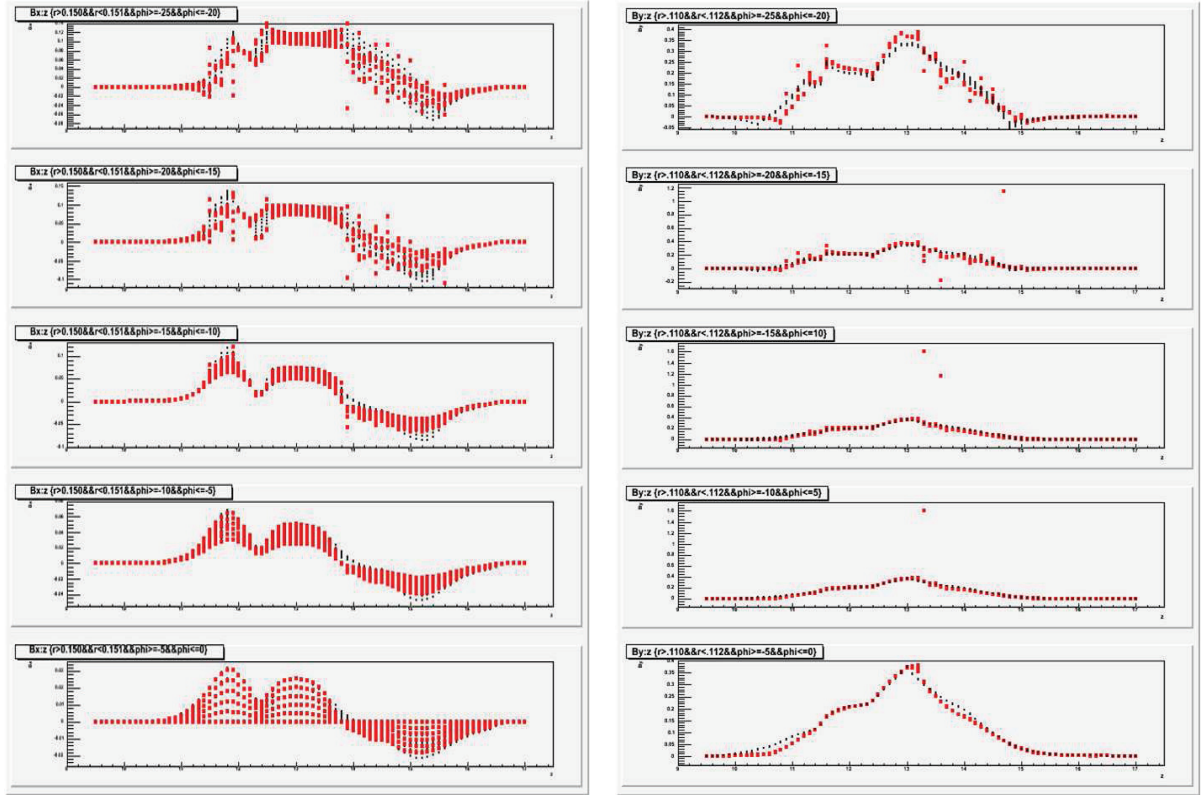


Figure B.3: The azimuthally focusing component (left) and radially focusing component (right) of the TOSCA (black) and original proposal (red) field maps vs. z at radius of 15 cm for different 5° portions of the azimuth from -25° to -20° (top), down to -5° to 0° (bottom).

B.3 Towards a More Realistic Magnet Design

In order to prepare for the first engineering review, held on August 31, 2010, a more realistic magnet design was developed using TOSCA. For the original proposal, the field map was produced using a Biot-Savart calculation of line currents. The design that was presented in the proposal consisted of four segments with different amounts of current in each segment. The amount of current increases going downstream. This is done in order to optimize the amount of field seen by the Møllers compared to the elastic ep scattered electrons. Because the electrons produced in the elastic ep process have more energy, there is some radial separation within the length of the magnet, and it can be designed so that in the segment at the end of the magnet (the one with the largest current) the Møller electrons are outside the inner radius of the coils, while the ep scattered electrons are below it and see much less field.

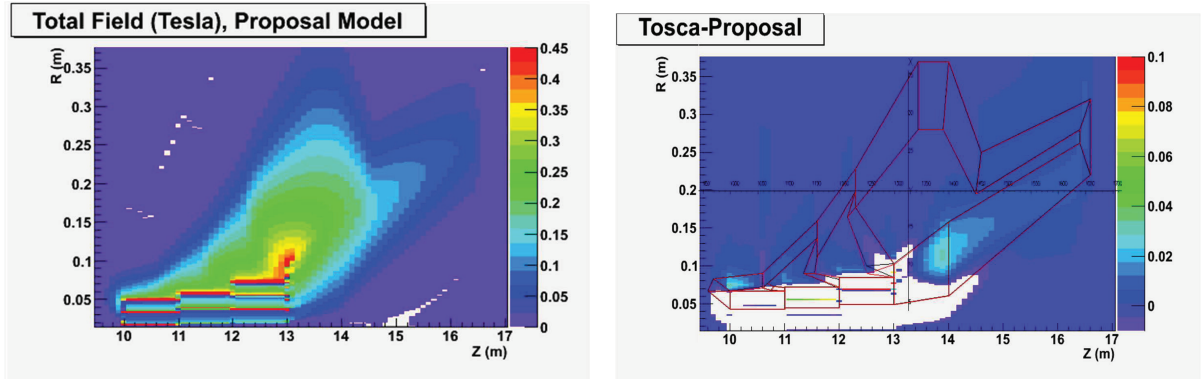


Figure B.4: The total average field in a sector for the proposal map is shown on the left. On the right is shown the difference (in Tesla) between the average fields in a sector for the TOSCA and original versions of the proposal, with the coil geometry superimposed. Non-zero differences arise due to slight differences in the actual geometrical definitions of the coils. The white region is where there are non-physical values of the field within the actual coil definition.

Any design of the magnet will have to utilize this feature.

The calculation of the field map optimized the current in each segment without taking into account the size of the conductor, which means that the currents in each segment and the difference in the currents from segment to segment were not necessarily integer multiples of any particular amount. TOSCA was used to define individual wire turns with actual dimension in a coil layout that included actual conductors with space for insulation. The first step in this process involved trying to fit wires of various sizes into the radial and azimuthal extent of the coils given by the proposal model and the relative currents between the different segments of the hybrid toroid. This resulted in a large number of out-of-plane bends to fit into a large ϕ extent (nearly the full azimuth) at low radius but transition to smaller than half of the azimuth at large radius.

Additional constraints that were taken into account in the design of the actual conductor layout include the minimum bend radius of the wires (5x the wire outer diameter (OD)) and the current density. The transition from the third segment into the most downstream segment, where the current is greatest and hence the number of wires is greatest, proved to be the limiting factor. The coils no longer fill the full azimuth at low radius along the whole length of the magnet, although they mostly fill it at this transition. The choice of conductor size did not seem to impact the current density, so an optimum conductor size was chosen based on whether the relative currents between segments was similar to the proposal.

This version of the hybrid torus (called version 1.0) produced physics results

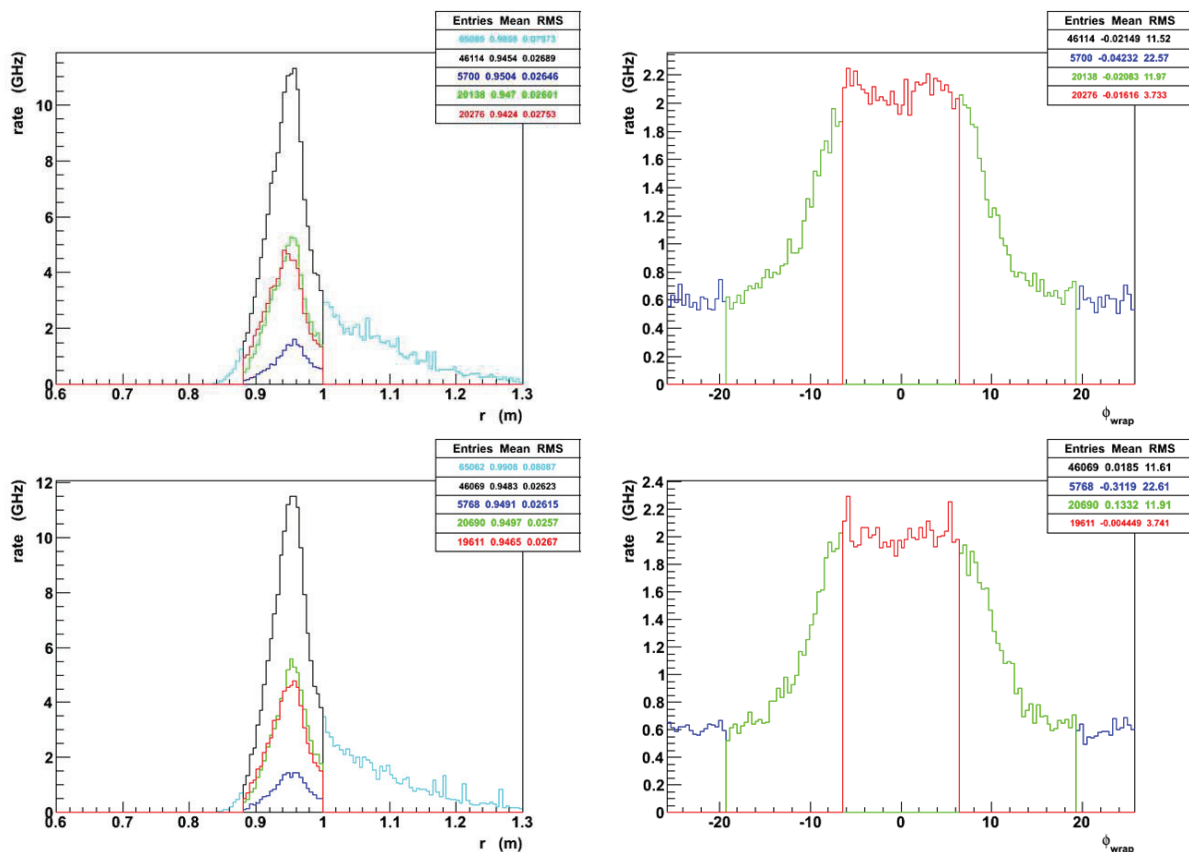


Figure B.5: The top two plots are from the GEANT4 results using the original proposal map, the bottom two plots used the TOSCA version of the proposal map. The plots on the left are for the radial distribution of events at the detector plane; the plots on the right show the ϕ location at the detector plane. The colors indicate whether the tracks are in the center of the open sector, the center of the closed sector, or straddle the open and closed sectors when they hit the detector plane (red, blue and green, respectively).

that were qualitatively similar to the proposal model. The radial focus occurs at a larger radius, which may be preferable for reducing photon backgrounds using shielding. Unfortunately it is also a bit wider, which adversely affects the background fraction from elastic ep electrons, and from other sources of background as well. According to GEANT4 simulations the Møller rate without optimizing the collimators is higher (see Table B.3), but so is the background from the elastic eps. Further work would be needed to optimize this version, including revisiting the collimation. However, this version was put aside in favor of one which takes into account the suggestions made by engineers during the first magnet review. Opti-

Table B.1: The number of wires and currents in the different segments based on the choice of conductor size. The segments under consideration are those that are defined as the inner radial parts of the coils in the different segments, with X being the most upstream, smallest current, and then Y, Z, and into A, which is the segment which contains the maximum current. The current density in each case is at least 1550 A/cm². The conductor with an OD of 0.4620 cm is the one presented at the magnet review. The last row is the one used based on the comments from engineers.

OD (cm)	A_{cond} (cm ²)	Total # Wires				Current (A)				\vec{J} (A/cm ²)
		X	Y	Z	A	X	Y	Z	A	
Proposal	—	—	—	—	—	7748	10627	16859	29160	1100
0.4115	0.1248	40	54	86	146	7989	10785	17176	29160	1600
0.4620	0.1568	32	44	70	120	7776	10692	17010	29160	1550
0.5189	0.1978	26	36	56	94	8066	11168	17372	29160	1568
0.5827	0.2476	20	28	40	76	7680	10752	15360	29184	1551

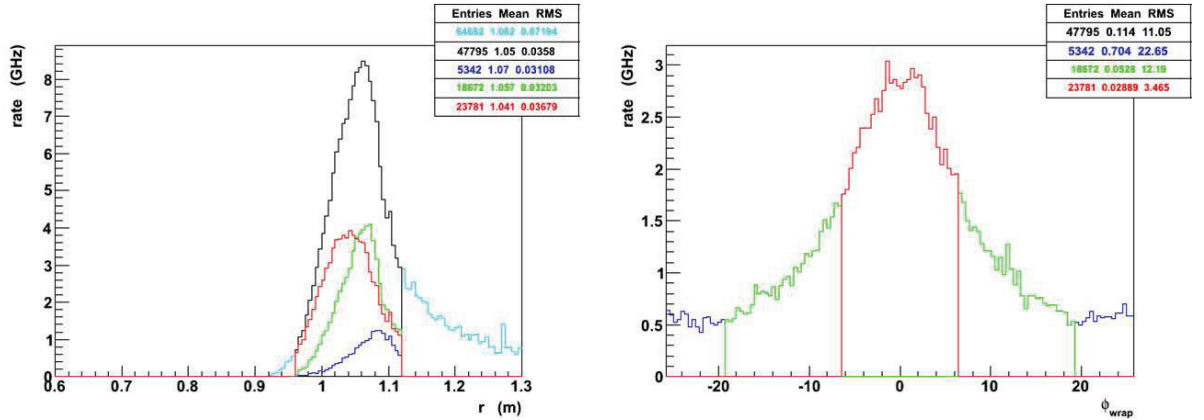


Figure B.6: Plots from GEANT4 simulations which used the field map produced using the actual conductor layout designed in TOSCA. The plot on the left is for the radial distribution of events at the detector plane; the plot on the right shows the ϕ location at the detector plane. The colors indicate whether the tracks are in the center of the open sector, the center of the closed sector, or straddle the open and closed sectors when they hit the detector plane (red, blue and green, respectively).

Table B.2: Comparison of various quantities for the two versions of the actual conductor layout. Concept 1 is what was presented at the magnet engineering review. Concept 2 takes into account suggestions made by the engineers at that meeting. *Note that the length is estimated for the longest turn only.

	Concept 1	Concept 2
weight_{coil} (lbs)	556	555
R_{coil} (Ohms)	1.98	0.741
V_{coil} (V)	480	285
I_{wire} (A)	243	384
P_{magnet} (kW)	820	765
\vec{J} (A/cm ²)	1600	1551
L_{turn} (m)	15*	15*
# turns	120	76

mization that as occurred as of the writing of this update for that version will be discussed in Section B.5.

B.4 Engineering Review

The first magnet review was very productive. The design as described in Section B.3 was presented to a panel of 6 engineers: George Clark (TRIUMF), Ernie Ihloff (MIT-Bates), Vladimir Kashikhin (Fermilab), Jim Kelsey (MIT-Bates), Dieter Walz (SLAC), and Robin Wines (JLab). In general the comments were positive and/or constructive, with nothing that would prevent the operation of the magnet, although there was no presentation of magnetic forces or a detailed study of positioning tolerances, which we hope will be available for the next magnet review, which is yet to be scheduled. The concerns that were raised involved water-cooling issues, including the size of the conductor/water-cooling aperture and the many bends in the design. Other issues included concerns about placing the coils around the “petal” vacuum volume and the lack of a support design. Requests for the next review, besides addressing these issues, included a better description of the geometry of the field (made difficult in part because of the hybrid nature of the magnet).

There was not much concern about the size of the current density in the coils, but rather more concern over the size of the water-cooling aperture. It was noted

that the water could simply be flowed faster and/or be chilled, but that the design with this small of a conductor would likely be too complicated to be realistic because there would be too many connections. It was a general consensus that a water-cooling hole of at least 0.125 inches would eliminate concerns about back-flows, eddies and build-up of oxides that could cause a plug and affect the long-term operation of the magnet. They agreed that the minimum bend radius should be 5x the conductor OD. It was suggested that a larger conductor may also reduce the “waves” down the length of the magnet that will be introduced during manufacture of the coils. We were cautioned against using two different conductor sizes, which would necessitate using different power supplies. So, the new design uses a larger conductor and has as few out-of-plane bends as possible, which results in about 38 water connections per coil (for supply and return).

A new design for the coils has been developed which takes into account these suggestions (see the last row in Table B.1). Because there are fewer conductors and they have a larger cross-section, the power in the magnet is slightly lower and the voltage per coil is almost half of what it was in the first actual conductor layout (see Table B.2). Optimization for physics optics results should not change the design of the magnet to the point where the support concept could not be easily adapted, so this updated version has been sent to JLab engineers for design of structural supports and water-cooling system. It was suggested during the meeting that the coils should be mounted inside the vacuum volume due both to space constraints and the complicated nature of the vacuum volume as proposed making it hard to be ASME compliant. The engineers suggested that it should be straightforward to stiffen the coils with G10 or carbon but cautioned that whatever epoxy or insulator we used would have to be radiation hard.

Work since the meeting has included estimates of the magnetic forces on the coils and determining keep-out zones which will help minimize the position sensitivities (which were taken into account in the updated design). The preliminary results from the study of the magnetic forces using TOSCA is that the centering force on the coils is about 3000 lbs., or 5500 lbs. on the inner part of the coil (inward) and 2600 lbs. on the outer part of the coil (outward). This can be compared to QTOR, the Qweak magnet, which has a centering force of 28,000 lbs. per coil (which was also verified within a factor of 2 using TOSCA). The effect of asymmetrically placed coils and coil motion upon being powered up need to be studied and taken into account in the design of the supports.

Some other suggestions that were made include the use of steel which would increase the field and decrease the forces, eliminating the lowest current, most upstream part of the magnet, checking the tolerances because of the large variation in the radially focusing field and the possibility of introducing iron poles in order to reduce the size of the coil cross-section. In general we want to avoid any magnetic material because of backgrounds, so the steel and the iron poles will be kept in reserve for now. The upstream part of the magnet helps to separate the Møllers and

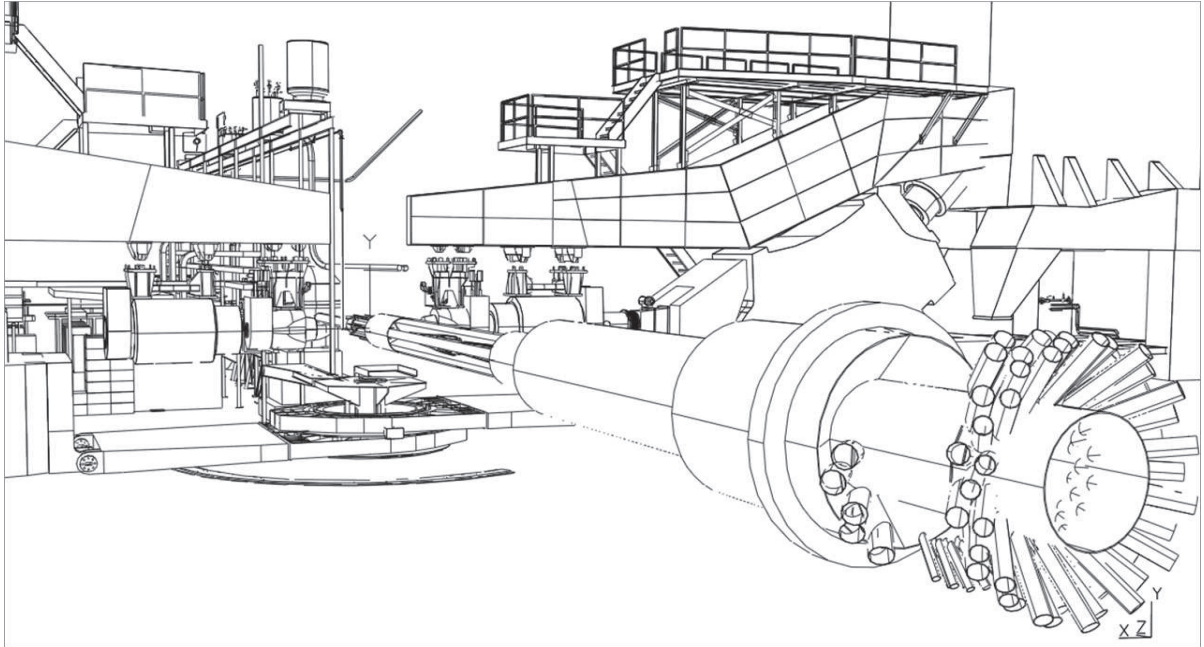


Figure B.7: Current design placed in Hall using TOSCA step file.

the electrons that underwent elastic ep scattering, so we need that in order to make the rest of the magnet more effective. A detailed sensitivity study will be done for a design that is more optimized from an optics point of view.

B.5 Optimizing for Physics Considerations

The design that was achieved for the proposal field map was very robust, and the qualitative performance was not too adversely sensitive to the initial changes in the coil geometry going from the line current model to an actual conductor layout. The first actual conductor layout was chosen specifically to keep the relative currents between segments as close to the proposal model as possible. As a result of the changes adopted to meet the engineers' recommendations, however, the optical properties of the magnets changed somewhat more significantly (see Figure B.10). It should be possible to optimize the magnet by making judicious changes that will maintain the necessary engineering aspects of the current design.

The optimization is faster than with the home built code. TOSCA is used to make the changes to the geometry, and tracks are generated which can be used to gauge the effect on unradiated Møller and elastic ep scattered electrons which have the correct energy-angle dependence (see Figure B.8). This is a relatively fast turn-around, making use of the "coils only" calculation due to the fact that so far, all of our materials are linear. If this were not the case, it would be necessary to use

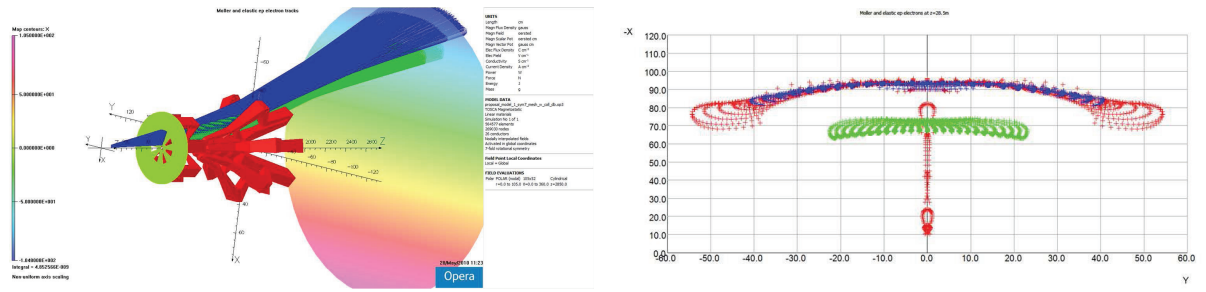


Figure B.8: The figure on the left shows Møller (blue) and elastic ep (green) tracks generated in TOSCA, with a collimator in place. The plot on the right shows the same tracks at the intersection of a plane at the detector location (Møller tracks with no collimation are shown in red).

the finite element analysis capabilities of TOSCA. A “blocky model” of the actual conductor layout is used to reduce the calculation time (see Figure B.9). Tracks for 3 geometries are generated simultaneously on a machine purchased by UMass for this purpose (the limit of 3 is due to the number of available licenses being 4, and leaving one open for use by another JLab user, not a limit of the machine itself). The tracks can be examined in 3 dimensions within the framework of TOSCA, which allows for the identification of interferences with the coils. They also can be plotted at the intersection of a plane which shows the X:Y distribution at the detector plane so that the separation between the ep and Møller peak can be taken into consideration.

The major difference between the proposal model and the model that takes into account the recommendations of the engineers is that the radial focus is a bit wider, which makes the background fraction higher (see Figure B.10). In order to explore the possibility of improving the radial focus, two changes to the geometry of the magnet were explored. One is to change the angle of the tail of the magnet to minimize the field seen by the elastic ep scattered electrons, while ensuring that the Møllers still see as much field as possible. In order to improve this, the field in the upstream magnet was increased (the current density with the increased field is 1202 A/cm^2). The other change is to reduce the radius of the outer part of the coil in order to minimize the field seen by the high angle scatters, thus focusing them better at the detector plane. This change has the adverse effect of reducing the separation between the ends of the Møller distribution and the elastic ep distribution.

The focus is somewhat better for Møllers with low scattering angles, which increased the overall Møller rate even in the first actual conductor layout compared to the proposal (see Table B.3). It should also be possible to trim the acceptance a bit, maintain a relatively high Møller rate but reduce the size of the radial distribution at the focal plane and thereby reduce the background fraction. The accepted angular range is also bigger than it needs to be from the point of few of full az-

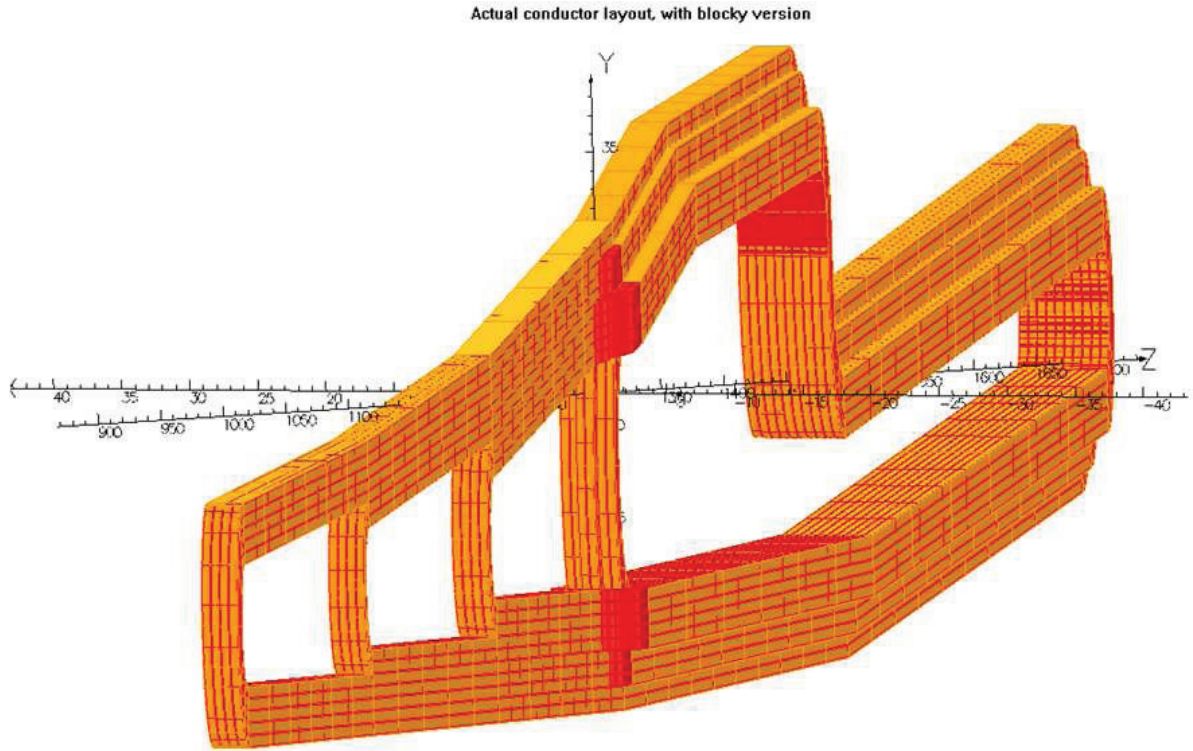


Figure B.9: The actual conductor layout of the model which has been updated to take into account the recommendations from the engineers as a result of the magnet review. The actual wires are shown in red, and the blocky model which is used in the optimization is shown in orange.

imutal acceptance. That is, we only really want high angle scatters that have a corresponding low angle “partner” accepted, as described above and in the original proposal in more detail.

As the optimization for physics considerations nears completion, it will be necessary to revisit the collimation, both from the point of view of reducing the angular acceptance based on the studies described above, but also to reduce the photon background. The collimation that is currently being used is the same as what was used in the original proposal and has not yet been optimized for the present magnet design. Once the optics have been optimized in TOSCA, the collimation will be optimized for that version, and if necessary the magnet design could be tweaked as well. The radial focus is at a larger radius, which should help from the point of view of shielding the photon background, and reducing the size of the radial focus should help as well.

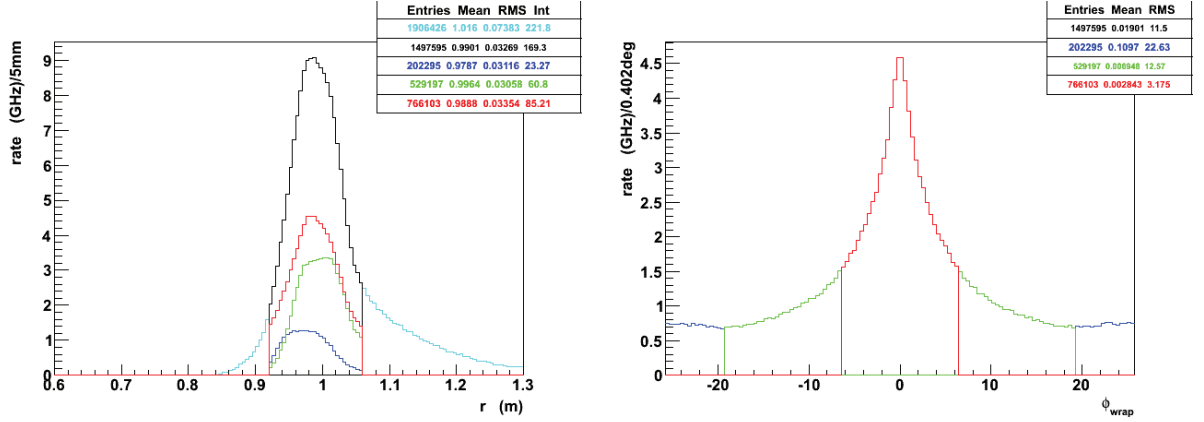


Figure B.10: Plots from GEANT4 simulations which used the field map for the design updated based on the feedback from the engineering review, after optics tweaks (version 2.6). The plot on the left is for the radial distribution of events at the detector plane; the plot on the right shows the ϕ location at the detector plane. The colors indicate whether the tracks are in the center of the open sector, the center of the closed sector, or straddle the open and closed sectors when they hit the detector plane (red, blue and green, respectively).

Table B.3: Estimated rates for various simulated processes in the radial bite chosen for the detectors, according to the GEANT4 simulation for different versions of the field maps. These numbers assume a beam current of $75 \mu\text{A}$.

Field Map	Møller (GHz)	Elastic ep (GHz)	Inelastic ep (GHz)	Bkgd. Fraction (%)
Proposal	133	12	0.4	9
Actual (v1.0)	162	28	0.6	10
Actual (v2.6)	169	25	0.8	13
Actual (v2.11)	171	24	0.8	13